Regional Studies in Marine Science 16 (2017) 116–123

Contents lists available at ScienceDirect

Regional Studies in Marine Science

journal homepage: www.elsevier.com/locate/rsma

Longshore wave energy flux: Variability and trends in the southern coast of Buenos Aires, Argentina

Iael Pérez [a,b,*], Guadalupe Alonso [a,c], Andrés Pescio [a,c], Walter Dragani [a,b,c,d], Jorge Codignotto [b,e]

[a] Servicio de Hidrografía Naval, Av. Montes de Oca 2124 (C1270ABV) Ciudad Autónoma de Buenos Aires, Argentina
[b] CONICET, Consejo Nacional de Investigaciones Científicas y Técnicas, Av. Rivadavia 1917, (C1033AAJ) Ciudad Autónoma de Buenos Aires, Argentina
[c] Departamento de Ciencias de la Atmósfera y los Océanos, Facultad de Ciencias Exactas y Naturales, UBA, Ciudad Universitaria, Pabellón II, 2do. Piso, (C1428EGA) Ciudad Autónoma de Buenos Aires, Argentina
[d] Instituto Franco-Argentino para el Estudio del Clima y sus Impactos (UMI IFAECI/CNRS–CONICET–UBA), Ciudad Universitaria, Pabellón II, 2do. Piso, (C1428EGA) Ciudad Autónoma de Buenos Aires, Argentina
[e] Servicio Geológico Minero Argentino (SEGEMAR), Av. Julio A. Roca 651 101 P (C1067ABB), Ciudad Autónoma de Buenos Aires, Argentina

ARTICLE INFO

Article history:
Received 7 November 2016
Received in revised form 3 August 2017
Accepted 3 August 2017
Available online 23 August 2017

Keywords:
Waves
Longshore energy flux
Climatic variability
Trends
Southern coast of Buenos Aires
Climatic indices

ABSTRACT

Variability and trends of the longshore wave energy flux were analyzed between Bahía Blanca and Mar del Plata, along the southern coast of Buenos Aires, Argentina. Longshore energy flux was assessed from wave parameters obtained from long-term numerical simulations carried out with a validated model (Simulated Waves Nearshore model) for the period 1979–2012. It was determined that the longshore energy flux flows predominantly eastwards. Mean values and standard deviations of the longshore flux increased eastwards. Two different areas were defined in the study region: the eastern area, characterized by higher values of longshore energy flux, and the western one, where fluxes were approximately 14% of the eastern values. Longshore wave energy flux did not present significant long term trends in the study region. High inter-annual variability in longshore wave energy flux was observed especially at the eastern area of the study region. Possible connections between this inter-annual variability and climatic indices related to El Niño / Southern Oscillation and the Southern Annual Oscillation were investigated. Significant correlation coefficients were obtained for both indices at the easternmost locations of the study region. This indicates that both climatic anomalies can impact on the wave climate and littoral processes along the southern coast of Buenos Aires.

1. Introduction

Every coastal management strategy requires, among other issues, adequate information about the wave climate (Delgado et al., 2012). Waves are an essential factor in the hydrodynamic and geomorphology of coastal regions, particularly on sandy beaches. This phenomenon not only suspends the sediments but also triggers nearshore currents that carry the suspended sediments along or across-shore (Dean and Dalrymple, 2002). Several works showed evident changes in the wind wave climate from a global and regional perspective. One of the global studies was carried out by Young et al. (2011) by means of 23 years of validated and calibrated altimeter data. They found a clear significant trend of increasing extreme wave height at high latitudes and more neutral conditions in equatorial regions. Moreover, using results from a community derived multi-model ensemble of wave-climate projections Hemer et al. (2013) found an increase in annual mean significant wave height over 7.1% of the global ocean, predominantly in the Southern Ocean, which is greater during austral winter (July–September; 8.8%). Within more regional studies, in the North Atlantic Ocean over the 20th century a significant increase in wave height was reported by Bertin et al. (2013), who developed a 109 year numerical wind-wave hindcast. For Latin America and the Caribbean region, Reguero et al. (2013) described the wave climatology based on the global wave reanalysis forced with the reanalysis from the National Center for Environmental Prediction/National Center for Atmospheric Research (NCEP/NCAR, Kalnay et al., 1996). Long-term changes were identified in the wave heights and mean direction of the energy flux, which showed high space variability. Finally, space and time variability of extreme wave climate was analyzed by Izaguirre et al. (2013).

The coast of the Buenos Aires (Fig. 1) is constituted almost entirely of sandy beaches, with seaside resorts crowded with tourists in the summer. The only exceptions are Mar del Plata

* Corresponding author at: Servicio de Hidrografía Naval, Av. Montes de Oca 2124, (C1270ABV) Ciudad Autónoma de Buenos Aires, Argentina.
E-mail address: iaelperez@gmail.com (I. Pérez).

http://dx.doi.org/10.1016/j.rsma.2017.08.002
2352-4855/

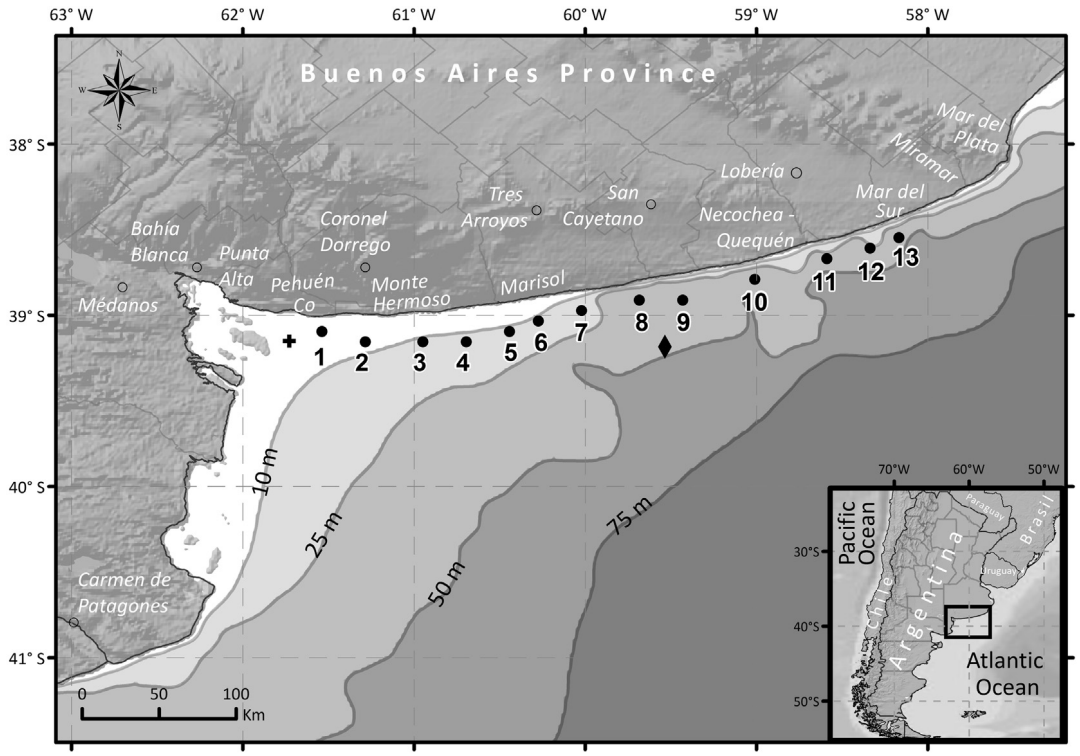

Fig. 1. The southern coast of Buenos Aires (Argentina) and its locations, in the southwestern Atlantic Ocean. Numbers indicate the position of the analyzed locations. The black cross indicates the position of the wave gauge located off-shore Pehuén-Co. The black diamond indicates the location where the validation between satellite and simulated significant wave height (Hs) trends was carried out.

and some areas of Quequén and Necochea where the coast is constituted by cliffs. The mean wave height along the coast slightly increases south-westwards and ranges from 1 m to 1.5 m (Dragani et al., 2010). The tide regime is mixed, predominantly semidiurnal (Balay, 1955) and the tidal range increases westwards (SHN, 2017), from Mar del Plata (0.83 m) to Bahía Blanca (2.62 m). Some particular beach resorts located along the southern coast of Buenos Aires (Fig. 1) are incurring natural erosive processes, which are aggravated by human activities including urbanization, foredune degradation and/or sand mining. In this regard, some authors reported an increase in the erosive processes along the coast of Buenos Aires during the last three decades of the 20th century. For instance, Kokot (1997) linked together the enhanced erosion with changes in atmospheric and oceanic processes which seem to be a consequence of climate change. The erosion process along the coast of Buenos Aires was also studied by Diez et al. (2007), who related it to increased sea level. Some particular areas of the southern coast of Buenos Aires are significantly affected by cliff erosion. Regarding this matter, Isla and Cortizo (2014) estimated a mean rate of cliff retreat of about 0.5/0.6 m/year, by comparing old photographs with modern satellite images. Moreover, a study of morphological changes along the coastline of Necochea and Quequén was carried out by Merlotto et al. (2013) through the analysis of aerial photographs, satellite images, and beach profiles. Even though some evidences of beach stability were observed at Necochea, the retreat of the coastline and a negative sedimentary balance at Quequén could indicate an accentuated erosion process. Furthermore, evident and progressive coastal changes produced by erosion are clear for the neighborhoods of Pehuén-Co and Monte Hermoso. These alterations are causing private capital losses and risks in nature and anthropologic reserves (Rojas et al., 2014).

Variation in wave climate could be the trigger of alterations in the littoral processes of the region. For this reason, Dragani et al. (2013) studied the wave climate employing numerical simulation with the SWAN model, along the northern coast of Buenos Aires. They found a significant increase of wave heights (S and SSE directions). Furthermore, this simulation presented an increase in the number of cases of waves coming from the S, SSE, and E.

Additionally, the area located between Pehuén-Co and Monte Hermoso has been designated as a geological, paleontological and archeological reserve and it may be declared a World Heritage Site by UNESCO. This region in particular constitutes a worldwide unique system due to the existence of anthropological and paleontological footprints (Perillo and Iribarne, 2003).

Despite the importance of the understanding of wave climate, its changes and impacts on the coast and its associated longshore energy flux, there are almost no systematic measurements of wind wave parameters between Bahía Blanca and Mar del Plata. There are only two relatively short wave data records: the first wave data series is currently being collected (since 2007, with a non-directional wave sensor) 21 km off-shore Pehuén-Co (Fig. 1). And the second wave data series were measured 500 m off-shore Quequén Port with a S4 Interocean current/wave meter. This last data record began in 2007 and presents several gaps, some of them significantly long. The lack of long-term, systematic and directional wave data series explains, in part, the scarce amount of scientific papers about longshore currents, near shore circulation, onshore/off-shore and longshore sediment transport (and their time and space variability) along the southern coast of Buenos Aires.

Perhaps the largest impact on coastal stability is caused by the variability or change of the longshore net sediment transport (Syvitski et al., 2005). It is assumed that the net transport of sand in the southern coast of Buenos Aires, between the estuary of Bahia Blanca and Mar del Plata, is predominantly from SW to NE (Perillo et al., 2005). This assumption is mainly supported by the progressive accumulation of sand observed on the western side of the western breakwater of Quequén Port. Nevertheless, the prevailing direction of the net sand transport is rather uncertain between Bahia Blanca estuary and Quequén Port. The absence of

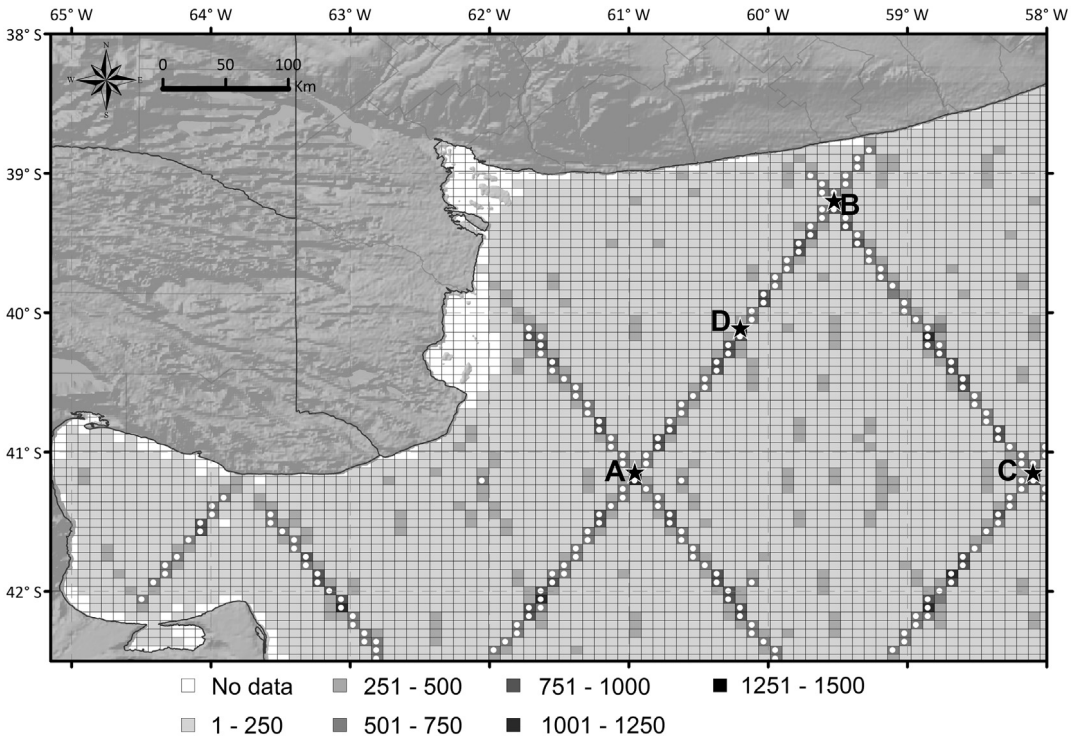

Fig. 2. High resolution model domain. The available amount of altimeter data (period: 1991–2012) is denoted for each grid cell. White circles indicate locations where simulated Hs were validated. Points A, B, C and D indicate locations where scatter plots between satellite data and simulated Hs are shown (see Fig. 3).

coastal structures along this coastal area – which usually provides a clear indication of the prevailing direction of the net transport – contributes to maintaining this uncertainty. However, it is largely known that the potential longshore sediment transport rate can be estimated from the longshore component of the wave energy flux in the surf zone (CERC, 1984). Therefore, the main objective of this work is to carry out an integral study of the longshore wave energy flux along the southern coast of Buenos Aires, between Bahia Blanca and Mar del Plata (Fig. 1). Long-term data series of wave parameters were simulated using SWAN (Simulated Waves Nearshore) model for the period 1979–2012. In addition, satellite data have not enough time/space resolution and are rather short for carrying out climatic studies. Annual longshore energy flux, (space and time) variability and trends were computed from simulated wave parameters at selected locations of the study area. The correlation between estimated annual energy flux and some climatic indices, usually adopted to describe the ENSO (El Niño/Southern Oscillation) and the SAM (Southern Annual Mode), are investigated and discussed in this paper.

2. Data and methods

2.1. Wave model

Wave parameters, annual longshore energy flux, and trends were derived from numerical simulations carried out with the SWAN model. This is a numerical wave model that provides realistic estimates of wave parameters in coastal areas (Booij et al., 1999; Ris et al., 1999; Holthuijsen et al., 2004). The implementation of the model to the study region spans the area between 38°S and 42. 5°S, and 58°W and 66°W, with a grid space resolution of 7 km × 7 km (75 × 96 grid points). The model domain is presented in Fig. 2. The boundary conditions were provided by a larger low resolution grid covering the area between 31°S and 47°S, and 45°W and 68°W, with a grid space resolution of 23 km × 23 km (77 × 87 grid points). It has been demonstrated (Dragani et al., 2008) that this extended domain is large enough to generate realistic wind wave fields (sea and swell) in the Buenos Aires coastal area.

The atmospheric forcing were the four daily fields (0, 6, 12 and, 18 GMT) of the 10 m wind components from the NCEP/NCAR Reanalysis I. This reanalysis has been successfully implemented as forcing in several numerical regional studies in the area (Simionato et al., 2005, 2006a, b, 2007; Dragani et al., 2010; Codignotto et al., 2012). A discussion about the quality of NCEP/NCAR I over the Southern Hemisphere can be found in Simmonds and Keay (2000), and a complete description of this reanalysis and its dataset can be found in Kalnay et al. (1996). Recently Pescio et al. (2016) showed that, even though the Climate Forecast System Reanalysis (CFSR) is a newer reanalysis with higher time and space resolution executed in a coupled mode, wind speed trends seem to be better reflected by the NCEP/NCAR I in the study area.

The model was run in a non-stationary mode, whereas the bathymetry was obtained as a combination of a depth dataset (space resolution: 0.0167° × 0.0167°) obtained from GEBCO (2003) for deep waters (>200 m) and digitized nautical charts for the continental shelf (SHN, 1986, 1992, 1993, 1999a, 1999b). The drag coefficient was modified according to Simionato et al. (2006a, b) and Dragani et al. (2008).

Numerical simulations were validated using in situ and satellite wave parameters. Firstly, modeled significant wave heights (Hs) were compared with altimeter Hs data available in the study area. The altimeter database was obtained from the Globwave Project (Queffeulou and Croizé-Fillon, 2013) and consists on calibrated Hs from eight missions: ERS-1, ERS-2, TOPEX-Poseidon, GEOSAT Follow-ON (GFO), Jason-1, Jason-2, ENVISAT and CryoSat, covering the 1991–2012 period. Altimeter data were gridded in order to match them to the implemented high resolution model grid. The available amount of satellite measurements corresponding to each grid cell is presented in Fig. 2. As it can be seen in that figure, the majority of the grid cells in the computational domain have very few altimeter data (less than 250 data) to carry out a satisfactory validation. Only grid cells with more than 750 altimeter data were

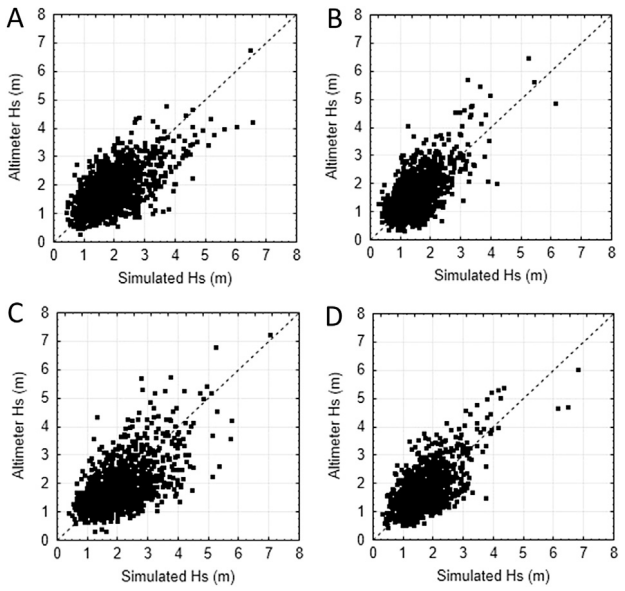

Fig. 3. Scatter plots between satellite and simulated Hs for selected grid cells. Locations are indicated with points A, B, C and D in Fig. 2.

considered. Then, approximately 200 grid cells were selected to perform the validation of the numerical simulations which are indicated with white circles in Fig. 2. Scatter plots between satellite and simulated Hs show a good agreement for the study region. Mean bias (measured Hs minus modeled Hs) resulted equal to 0.04 m, mean scatter index (root mean square error to mean measured Hs ratio) was 0.37 and mean correlation index was 0.61. Scatter plots for the four grid cells with more altimeter data (namely A, B, C, and D in Fig. 2) are presented in Fig. 3. On the other hand, simulated Hs were compared with observed Hs measured near Bahía Blanca (Fig. 1) in the period 2007–2011. This period was selected because it presents a minimal amount of gaps. The resulting bias (0.11 m), scatter index (0.52) and correlation index (0.55) indicated a good performance of the numerical simulations. Wave data gathered near the mouth of Quequén Port were not used for validation because they were obtained very close to the coast. In addition trends in simulated wave parameters were also validated against altimeter wave height data trends for the period 1992–2012. Trends for altimeter data and modeled wave heights are presented for the node B (Fig. 2) which is the node closest to the coast in the study region. As a result, computed trends were very similar: +7.3 mm/decade for modeled wave heights and +7.7 mm/decade for altimeter wave parameters.

2.2. Longshore wave energy flux

The statement that the prevailing direction of the net sand littoral transport is eastwards at Quequén, with a maximum estimated value of 1.3 10^6 m^3 yr^{-1}, is supported by few observations (Framiñan, 1990). Nevertheless, there is some uncertainty about the predominant direction of the littoral transport in the coastal area located at the west of Quequén, between Monte Hermoso and Bahía Blanca. The potential longshore sediment transport can be considered proportional to the longshore wave energy flux per unit crest (Pl) given by:

$$Pl = 0.05\rho g^{3/2} Hs^{5/2} (\cos\alpha)^{1/4} (\sin 2\alpha) \quad (1)$$

which was recommended by CERC (1984). In this expression ρ is the density of seawater (constant, equal to 1030 kg m^{-3}), g the acceleration due to gravity (9.86 m s^{-2}), Hs the significant wave height and α the wave angle between the wave crest and the shoreline, both wave parameters corresponding to deep waters. The predominant orientation of the shoreline was estimated from Landsat images (Data SIO, NOAA, US Navy, NGA, GEBCO, source: Google Earth, 2016). The orientation of the shoreline (respect to a geographic parallel) ranges from 0° (W–E) on the west area of the study region to 33°(SW–NE) on the east area. Computed Pl can be positive (eastward) or negative (westward) depending on the instantaneous value of α. Accordingly, annual net Pl (Pl_N, the sum of the individual Pl in a year) can also result in an eastward direction (positive) or a westward direction (negative). Annual western Pl (Pl_W, the sum of the negative Pl in a year) and annual eastern Pl (Pl_E, the sum of the positive Pl in a year) were also obtained.

3. Results

Simulated Hs (period: 1979–2012) were analyzed for thirteen selected locations placed between Pehuén-Co and Mar del Sur (Fig. 1). Mean Hs increases eastwards, from 0.60 to 1.20 m, and maximum Hs also increases eastwards reaching values up to 6.3 m close to Mar del Sur. Waves predominantly propagate northwards in this region (25% of cases). Trends in wind wave heights were analyzed in the study area. Significant positive trends were detected near Mar del Plata (points: 11, 12 and 13) reaching maximum values of +16 mm/decade. In addition, trends in wave heights (Hs) were also studied considering the eight main directions (N: for waves coming between 337.5° and 22.5°, NE: between 22.5° and 67.5°, E: between 67.5° and 112.5°, and so on). Trends in Hs were statistically different from zero only for the E and NE directions. Computed trends, for waves coming from the E and NE, are ranged from +8 and +23 mm/decade and from +8 and +31 mm/decade, respectively. In order to illustrate these trends, simulated mean annual Hs and fitted regression lines (which show the mean trends) for waves coming from the E and NE, for locations 1 and 9, are presented in Fig. 4. Mean annual Hs and fitted regression lines corresponding to other locations are similar to them and are not included in this work. Computed trends for directional frequency of occurrence (number of cases per year, for the eight directions) were also studied. Negative trends (significantly different from zero, with 95% confidence) were obtained for waves coming from the SW for all analyzed locations. Negative trends were also obtained for waves propagating from the NW, but they were slightly smaller than trends for waves propagating from SW and are only significantly different from zero at locations 11, 12 and 13.

Average Pl_N were calculated for the period 1979–2012 ($Pl_{N\text{-}AVE}$) which resulted in a predominantly eastward direction (Fig. 5). Subsequently, this last fact supports that the annual rate of the potential longshore transport would be mainly eastwards between Bahía Blanca and Mar del Plata. $Pl_{N\text{-}AVE}$ increases eastwards, from a null value at location 1 to a maximum value (2150 J m^{-1} s^{-1}) at location 13. $Pl_{N\text{-}AVE}$ was virtually negligible (not statistically different from zero) at sites 2 and 5, located in the western zone of the study region. Westward and eastward averaged Pl ($Pl_{W\text{-}AVE}$ and $Pl_{E\text{-}AVE}$, respectively) were also computed for the period 1979–2012. $Pl_{W\text{-}AVE}$ and $Pl_{E\text{-}AVE}$ are represented with arrows and the values (in J m^{-1} s^{-1}) of $Pl_{N\text{-}AVE}$ are included in Fig. 5. In the western zone, $Pl_{N\text{-}AVE}$ is one or two orders of magnitude smaller than the values corresponding to the eastern zone, where $Pl_{N\text{-}AVE}$ is towards the E. Consequently, taking into account the computed values of $Pl_{N\text{-}AVE}$, the thirteen locations analyzed were preliminarily clustered in two different groups: the western (locations 1 to 7) and eastern groups (locations 8 to 13). The western locations presented relatively low values of $Pl_{N\text{-}AVE}$ (160 J m^{-1} s^{-1}) while the eastern locations showed values approximately ten times greater (1650 J m^{-1} s^{-1}). Values of Pl_N are presented for each location in Fig. 6.

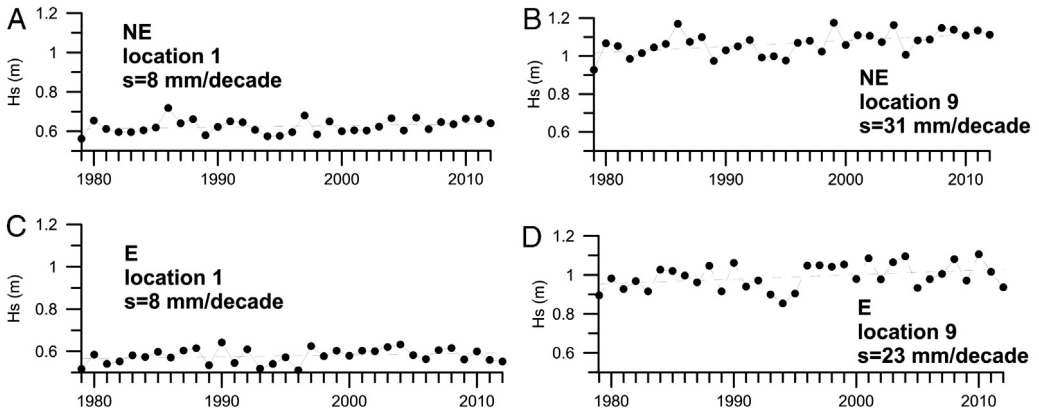

Fig. 4. Mean annual Hs (period: 1979–2012) for waves coming from NE (A–B) and E (C–D) for point 1 (A–C) and point 9 (B–D). Least-square regression (dashed) line and trends (mm/decade) are also included.

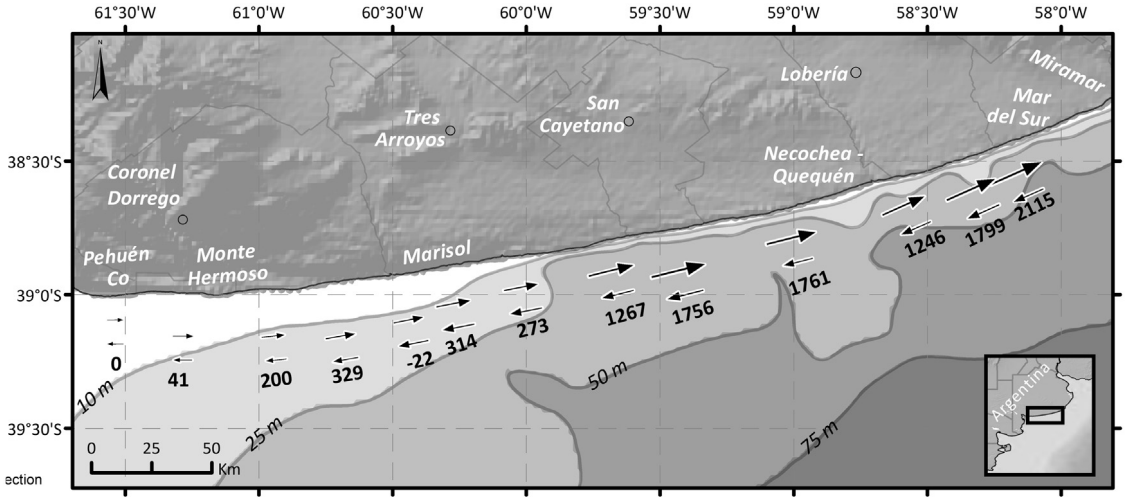

Fig. 5. Averaged annual westward and eastward Pl (period: 1979–2012) are indicated with arrows. Values of $Pl_{N\text{-}AVE}$ are also presented (in J m^{-1} s^{-1}), positive values correspond to eastward $Pl_{N\text{-}AVE}$.

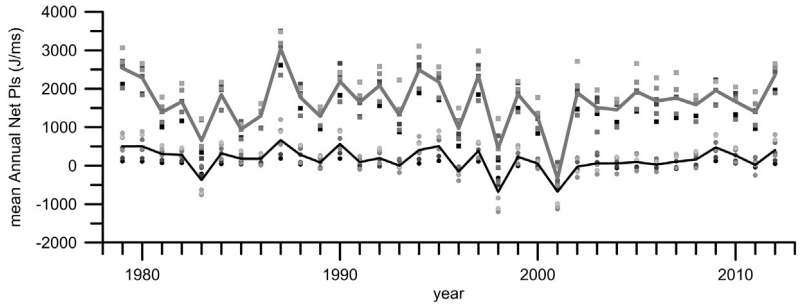

Fig. 6. Pl_N data series for thirteen analyzed locations (period 1979–2012). Averaged Pl_N for locations clustered in the western group (locations 1 to 7, black line) and in the eastern group (locations 8 to 13, gray line) are also included.

Averaged Pl_N for the western group of locations (1 to 7, black line) and for the eastern group (8 to 13, gray line) are also shown in Fig. 6. It can be noted that differences between western and eastern Pl_N are minimal for the years 1983, 1998 and 2001. This issue will be particularly discussed in the next section. A linear fit was carried out between pairs of western and eastern averaged Pl_N corresponding to the period 1979–2012. Pl_N for the years 1983, 1998 and 2001 were excluded from this analysis because they were considered atypical. The computed slope of the linear fit was equal to 0.14. This stated that the western averaged Pl_N is approximately 14% of the eastern averaged Pl_N. Pl_N and Pl_E data series do not present significant trends in the study region (locations 1 to 13, period: 1979–2012). In contrast, Pl_W data series showed significant negative trends at locations 3 to 6, which ranged from −30 to −70 Jm^{-1} s^{-1}/decade.

Standard deviations of Pl_N data series (SD_{PLN}) were computed for every location. The eastern group of locations presented SDPLN twice as large as the values assessed for the western group (650 and 300 Jm^{-1} s^{-1}, respectively). In addition, correlation coefficients were computed for all possible pair combinations of Pl_N data series corresponding to the thirteen locations of the study area. Then, 78

correlation coefficients (r_{i-j}) were obtained, where r_{i-j} is the correlation coefficient computed between data series corresponding to locations i and j ($1 \leq i \leq 13$, $1 \leq j \leq 13$, $i \neq j$ and $r_{i-j} = r_{j-i}$). All correlation coefficients were significantly different from zero and inversely proportional to the distance between different locations. Correlation coefficients for western locations (1–7) ranged from 0.86 to 0.99 and for the eastern locations (8–13) from 0.85 to 0.99. The lowest coefficient was obtained for correlation computed between locations 2 and 13 ($r_{2-13} = 0.51$). Then, even though Pl_N data series can be clustered into two defined groups, all of them (locations 1 to 13) presented fairly similar inter-annual variability.

4. Discussion

Annual net longshore energy flux and its (space and time) variability and trends were inferred from long-term numerical simulations carried out with the validated SWAN model at the southern coast of Buenos Aires. It is important to highlight that there are not regional antecedents in the peer reviewed scientific literature about this subject. Numerical simulations carried out in this work have shown that the wave climate is significantly different between the northern and southern coast of Buenos Aires. The most frequent wave direction is from the S (around 25% of cases) in the southern coast of Buenos Aires. But, wave direction in the Río de la Plata mouth, located approximately 600 km northeastwards from the study area, is rather different: from the SE (41%), E (28%) and S (14%) (Dragani and Romero, 2004). In addition, significant positive wave height trends, for the E and NE directions, and significant negative trends in the frequency of occurrence, only for the SW direction, were found on the southern coast of Buenos Aires.

Pl_N were calculated from simulated wave parameters for the period 1979–2012. Predominant eastward values of $Pl_{N\text{-}AVE}$ were obtained and, consequently, the rate of the potential sediment transport would be also positive (eastwards) and would increase towards the E. This fact is consistent with some visual evidences of accumulation of sand (for example, at Quequén Port) and with some preliminary studies carried out at Mar del Plata, located approximately 200 km east-northeastwards from Quequén. For example, Caviglia et al. (1991) estimated a north-eastward sediment transport rate ranged from 0.3 to 1.0 $\times$ 10^6 m^3 yr^{-1} at Mar del Plata. More recently, Dragani et al. (2013) inferred a north-northeastward direction and negative trends (approximately −20% per decade) for Pl_N at Pinamar, located around 100 km north-eastward Mar del Plata. On the contrary, no significant trend for Pl_N and Pl_E were inferred in the southern coast of Buenos Aires. However slight but significant negative trends for Pl_W (−2.5% per decade) were obtained at locations 3–7 placed in the western zone of the study area.

$Pl_{N\text{-}AVE}$ increases towards the E, but not regularly. $Pl_{N\text{-}AVE}$ increases abruptly from 273 to 1267 J m^{-1} s^{-1} from location 7–8, that is, at the border between the western and eastern clusters. Consequently, the rate of the potential longshore sediment transport would be significantly greater at location 8 than at location 7. The longshore sediment transport budget can be studied in a control volume defined between two transects normal to the coast in the surf zone. The on-shore/off-shore sediment transport is not taken into account in this preliminary analysis. For instance, if a control volume containing locations 7 and 8 is considered, the alongshore sediment budget will be negative and then the coast will be under an important erosive process. Differential imbalances like these in the longshore sediment transport could be a reasonable and preliminary explanation for the reported natural erosion along the southern coast of Buenos Aires (Rojas et al., 2014). For instance, observational evidences show that Marisol (Fig. 5) is clearly an erosive beach. It could be explained because $Pl_{N\text{-}AVE}$ presents a noticeable divergence between locations 5 and 6, −22 and 314 J m^{-1} s^{-1}, respectively. The alongshore sediment transport is westwards at location 5 and eastwards at 6 and consequently, the coast is under considerable erosive processes.

High inter-annual variability in Pl_N data series, especially at points clustered at the eastern group, can be clearly appreciated in Fig. 6. Even though Pl_N is usually positive, negative values can be observed for years 1983, 1998 y 2001. These anomalous values of Pl_N are possibly associated with atypical values in wave directions. Unusually high frequencies of occurrence were found for waves coming from the SE in 1998 and 2001, which are directly associated to negative values of Pl_N. These anomalous wave directions could probably be linked to regional variability in the surface wind circulation. Thus, possible relationships between the inter-annual variability in Pl_N and two climatic indices were investigated.

The ENSO (El Niño–Southern Oscillation) cycle refers to the coherent and sometimes very strong year-to-year variations in sea-surface temperatures, convective rainfall, surface air pressure and atmospheric circulation that occur across the equatorial Pacific Ocean (http://www.cpc.noaa.gov/products/analysis_monitoring/ensostuff/ensofaq.shtml#NINO). The Climate Prediction Center (http://www.cpc.noaa.gov) reported that two of the more intense ENSO events occurred in 1982–1983 and 1997–1998. Correlation coefficients between the Pl_N data series and the Southern Oscillation Index (SOI) were calculated and showed significant correlation (95% confidence level) for the easternmost locations of the study region (from 10 to 13). The maximum correlation coefficient was obtained at location 13 (0.52).

The SAM (Southern Annual Oscillation) is one of the annular modes of variability. It describes the north–south movement of the westerly wind belt (http://www.bom.gov.au/climate/enso/history/ln-2010-12/SAM-what.shtml). Correlation coefficients between the Pl_N data series and the SAM index were assessed and showed significant correlation (95% confidence level) for the easternmost locations of the study region (from 9 to 13). The maximum correlation coefficient was also obtained at the easternmost location (0.53). A comparison between normalized energy flux series with SOI and SAM indices are presented in Figs. 7 and 8, respectively. Normalized Pl_N series and SOI present a good agreement. Some differences can be seen between 1979 and 1985 and between 1999 and 2001 (Fig. 7). Normalized Pl_N series and SAM index also present a good agreement. The main differences can be appreciated at the beginning of the period, between 1979 and 1983 (Fig. 8).

5. Conclusion

Space and time variability of the longshore energy flux, estimated from a validated wave numerical model (SWAN), was investigated along the southern coast of Buenos Aires. Results have shown that the wave climate along the southern coast of Buenos Aires is significantly different from the wave climate along the northern coast. The most frequent wave direction is northwards (around 25% of the cases). Significant positive wave height trends (for E and NE directions) and significant negative trends in the frequency of occurrence (for SW direction) were found along the southern coast. Average Pl_N is predominantly eastwards and increases from W to E in the study region (Fig. 5). Subsequently, the rate of the potential annual longshore transport would be mainly eastwards between Bahía Blanca and Mar del Plata. $Pl_{N\text{-}AVE}$ and Pl_N standard deviations computed from the data series located in the eastern zone are significantly greater than values corresponding to data series in the western zone. Consequently, the thirteen analyzed locations can be clustered in two groups: the western (locations 1–7) and eastern groups (locations 8–13). $Pl_{N\text{-}AVE}$ increases abruptly from 273 to 1267 J m^{-1} s^{-1}, from location 7 to 8. Therefore, the rate of the potential longshore sediment transport would be significantly greater at location 8 than at location 7.

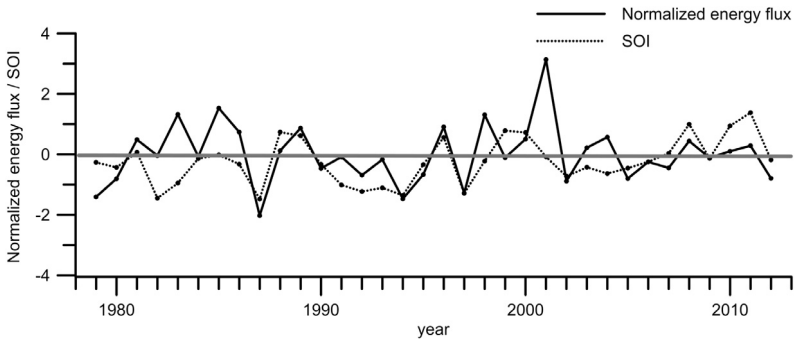

Fig. 7. Normalized Pl_N and SOI series for location 13.

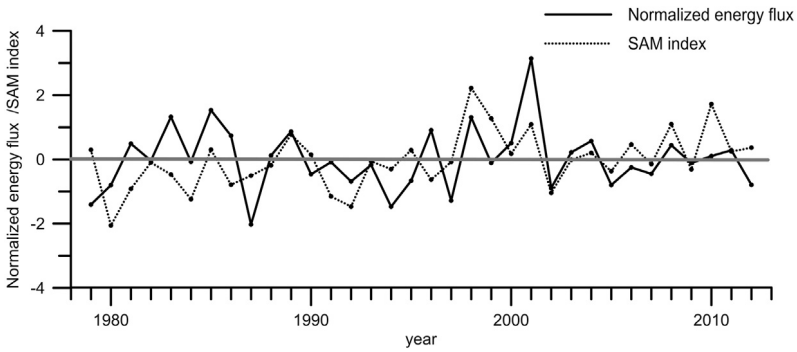

Fig. 8. Normalized Pl_N and SAM index series for location 13.

These imbalances in the longshore sediment transport could be a reasonable and preliminary explanation for the reported natural erosion along the southern coast of Buenos Aires.

Correlation coefficients were computed for all possible pairs of combinations of Pl_N data series corresponding to the thirteen locations. All correlation coefficients were significantly different from zero and inversely proportional to the distance between locations. Then, even though data series of Pl_N can be clustered into two defined groups, all of them seem to show fairly similar inter-annual variability. High inter-annual variability in the Pl_N data series can be noticed at locations clustered in the eastern group (Fig. 6). Possible connections between the inter-annual variability and climatic indices related to ENSO and SAM were investigated. Significant correlation coefficients (greater than 0.5) were obtained for both indices at the easternmost locations of the study region. This indicates that both climatic anomalies would impact on the wave climate along the southern coast of Buenos Aires.

Acknowledgment

This paper is a contribution to the CONICET PIP 112-201501-00174-CO project.

References

Balay, M., 1955. La determinación del nivel medio del Mar Argentino, influencias de las oscilaciones del mar no causadas por la marea, Dir Gral de Nav. Hidrog, Min de Mar.

Bertin, X., Prouteau, E., Letetrel, C., 2013. A significant increase in wave height in the North Atlantic Ocean over the 20th century. Glob. Planet. Change 106, 77–83. http://dx.doi.org/10.1016/j.gloplacha.2013.03.009.

Booij, N., Ris, R.R.C., Holthuijsen, L.H.L., 1999. A third-generation wave model for coastal regions 1. Model description and validation. J. Geophys. Res. 104, 7649–7666. http://dx.doi.org/10.1029/98jc02622.

Caviglia, F., Pousa, J., Lanfredi, N., 1991. A determination of the energy flux constant from dredge records. J. Coast. Res. 7, 543–549.

CERC, 1984. Shore Protection Manual, 1. Coastal Engineering Research Center. Department of Army, US Army Corps of Engineers, Washington, DC.

Codignotto, J.O., Dragani, W.C., Martin, P.B., Simionato, C.G., Medina, R.A., Alonso, G., 2012. Wind-wave climate change and increasing erosion in the outer Río de la Plata, Argentina. Cont. Shelf Res. 38, 110–116. http://dx.doi.org/10.1016/j.csr.2012.03.013.

Dean, R., Dalrymple, R., 2002. Coastal processes with engineering applications. Water. http://dx.doi.org/10.2277/0521602750.

Delgado, A.L., Vitale, A.J., Perillo, G.M.E., Piccolo, M.C., 2012. Preliminary analysis of waves in the coastal zone of Monte Hermoso and Pehuén Co, Argentina. J. Coast. Res. 283, 843–852. http://dx.doi.org/10.2112/JCOASTRES-D-10-00136.1.

Diez, P.G., Perillo, G.M.E., Piccolo, M.C., 2007. Vulnerability to sea-level rise on the coast of the Buenos Aires province. J. Coast. Res. 231, 119–126. http://dx.doi.org/10.2112/04-0205.1.

Dragani, W.C., Garavento, E., Simionato, C.G., Nuñez, M.N., Martin, P., Campos, M.I., 2008. Wave Simulation in the Outer Río de la Plata Estuary : Evaluation of SWAN Model, pp. 299–305.

Dragani, W.C., Martin, P.B., Alonso, G., Codignotto, J.O., Prario, B.E., Bacino, G., 2013. Wind wave climate change: Impacts on the littoral processes at the Northern Buenos Aires Province Coast, Argentina. Clim. Change 121, 649–660. http://dx.doi.org/10.1007/s10584-013-0928-8.

Dragani, W.C., Martin, P.B., Simionato, C.G., Campos, M.I., 2010. Are wind wave heights increasing in south-eastern South American continental shelf between 32°S and 40°S? Cont. Shelf Res. 30, 481–490. http://dx.doi.org/10.1016/j.csr.2010.01.002.

Dragani, W.C., Romero, S.I., 2004. Impact of a possible local wind change on the wave climate in the upper Río de la Plata. Int. J. Climatol. 24, 1149–1157. http://dx.doi.org/10.1002/joc.1049.

Framiñan, M., 1990. Transporte de sedimentos en Pinamar, Provincia de Buenos Aires. II Jornadas de Oceanografía Física y XVI Reunión Científica de Geofísica y Geodesia de la Asociación Argentina de Geofísicos y Geodestas, 15 pp., Bahía Blanca.

GEBCO, 2003. User guide to the centenary edition of the GEBCO Digital Atlas and its data sets. In: Jones, M.T. (Ed.), Natural Environment Research Council.

Hemer, M.A., Fan, Y., Mori, N., Semedo, A., Wang, X.L., 2013. Projected changes in wave climate from a multi-model ensemble. Nat. Clim. Change 3, 471–476. http://dx.doi.org/10.1038/nclimate1791.

Holthuijsen, L., Booij, N., Ris, R.C., Haagsma, L.G., Kieftenurg, A.T.M.M., Kriezi, E.E., Zijlema, M., Van der Westhuysen, A.J., Padilla-Herna´ndez, R., Rogers, E., Kaihatu, J., Petit, H., Campbell, T., Cazes, J., Hashimoto, N., 2004. Swan Cycle III Version 40.31, User Manual. Delft University of Technology, Faculty of Civil Engineering and Geosciences. Environmental Fluid Mechanics Section, Delft.

Isla, F.I., Cortizo, L.C., 2014. Sediment input from fluvial sources and cliff erosion to the continental shelf of Argentina. J. Integr. Coast. Zo. Manag. - Rev. GestãO Costeira Integr. 14, 553–568. http://dx.doi.org/10.5894/rgci472.

Izaguirre, C., Méndez, F.J., Espejo, A., Losada, I.J., Reguero, B.G., 2013. Extreme wave climate changes in Central-South America. Clim. Change 119, 277–290. http://dx.doi.org/10.1007/s10584-013-0712-9.

Kalnay, E., Kanamitsu, M., Kistler, R., Collins, W., Deaven, D., Gandin, L., Iredell, M., Saha, S., White, G., Woollen, J., Zhu, Y., Chelliah, M., Ebisuzaki, W., Higgins, W., Janowiak, J., Mo, K.C., Ropelewski, C., Wang, J., Leetmaa, A., Reynolds, R., Jenne, R., Dennis, J., 1996. The NCEP/NCAR 40-Year Reanalysis Project. Bull. Am. Meteorol. Soc..

Kokot, R.R., 1997. Littoral Drift, Evolution and Management in Punta Médanos, Argentin. J. Coast. Res. 20, 214–233.

Merlotto, A., Bértola, G.R., Isla, F.I., Cortizo, L.C., Piccolo, M.C., 2013. Short and medium-term coastal evolution of Necochea Municipality, Buenos Aires province, Argentina. Environ. Earth Sci. 71, 1213–1225. http://dx.doi.org/10.1007/s12665-013-2525-6.

Perillo, G.M.E., Iribarne, O.O., 2003. New mechanisms studied for creek formation in tidal flats: From crabs to tidal channels. Eos. Trans. Am. Geophys. Union 84, 1. http://dx.doi.org/10.1029/2003EO010001.

Perillo, G.M.E., Pérez, D.E., Piccolo, M.C., Palma, E.D., Cuadrado, D.G., 2005. Geomorphologic and physical characteristics of a human impacted estuary: Quequén Grande River Estuary, Argentina. Estuar. Coast. Shelf Sci. 62, 301–312. http://dx.doi.org/10.1016/j.ecss.2004.09.018.

Pescio, A.E., Martin, P.B., Dragani, W.C., 2016. Winds speed trends over the south-western Atlantic Ocean, between 33°and 50°S. Int. J. Climatol. 36, 501–507. http://dx.doi.org/10.1002/joc.4348.

Queffeulou, P., Croizé-Fillon, D., 2013. Global altimeter SWH data set - May 2013. Laboratoire d'Océanographie Spatiale, IFREMER, Plouzané, Francia.

Reguero, B.G., Méndez, F.J., Losada, I.J., 2013. Variability of multivariate wave climate in Latin America and the Caribbean. Glob. Planet. Change 100, 70–84. http://dx.doi.org/10.1016/j.gloplacha.2012.09.005.

Ris, R.C., Holthuijsen, L.H., Booij, N., 1999. A third-generation wave model for coastal regions 2. Verification. J. Geophys. Res. 104, 7667–7681.

Rojas, M.L., Recalde, M.Y., London, S., Perillo, G.M.E., Zilio, M.I., Piccolo, M.C., 2014. Behind the increasing erosion problem: The role of local institutions and social capital on coastal management in Argentina. Ocean Coast. Manage. 93, 76–87. http://dx.doi.org/10.1016/j.ocecoaman.2014.03.010.

SHN, 1986. Mar Argentino, de Río de la Plata al Cabo de Hornos. Nautical Chart 50, fourth ed. Servicio de Hidrografía Naval, Buenos Aires, Argentina.

SHN, 1992. Acceso al Río de la Plata. Nautical Chart H1, fifth ed. Servicio de Hidrografía Naval, Buenos Aires.

SHN, 1993. El Rincón, Golfo San Matías y Nuevo. Nautical Chart H2, fourth ed. Servicio de Hidrografía Naval, Buenos Aires.

SHN, 1999a. Río de la Plata Medio y Superior. Nautical Chart H116, fourth ed. Servicio de Hidrografía Naval, Buenos Aires.

SHN, 1999b. Río de la Plata Exterior. Nautical Chart H113, second ed. Servicio de Hidrografía Naval, Buenos Aires.

SHN, 2017. Tablas de Marea. Publicación H-610. Servicio de Hidrografía Naval, Buenos Aires.

Simionato, C.G., Meccia, V.L., Dragani, W.C., Guerrero, R., Nuñez, M., 2006a. Río de la Plata estuary response to wind variability in synoptic to intraseasonal scales: Barotropic response. J. Geophys. Res. Oceans 111, 1–14. http://dx.doi.org/10.1029/2005JC003297.

Simionato, C.G., Meccia, V.L., Dragani, W.C., Nuñez, M.N., 2006b. On the use of the NCEP/NCAR surface winds for modeling barotropic circulation in the Río de la Plata Estuary. Estuar. Coast. Shelf Sci. 70, 195–206. http://dx.doi.org/10.1016/j.ecss.2006.05.047.

Simionato, C.G., Meccia, V.L., Guerrero, R., Dragani, W.C., Nuñez, M., 2007. Río de la Plata estuary response to wind variability in synoptic to intraseasonal scales: 2. Currents' vertical structure and its implications for the salt wedge structure. J. Geophys. Res. Oceans 112, 1–15. http://dx.doi.org/10.1029/2006JC003815.

Simionato, C.G., Vera, C.S., Siegismund, F., 2005. Surface wind variability on seasonal and interannual scales over Río de la Plata area. J. Coast. Res. 21, 770–783. http://dx.doi.org/10.2112/008-NIS.1.

Simmonds, I., Keay, K., 2000. Mean southern hemisphere extratropical cyclone behavior in the 40-year NCEP-NCAR reanalysis. J. Clim. 13, 873–885. http://dx.doi.org/10.1175/1520-0442(2000)013<0873:MSHECB>2.0.CO;2.

Syvitski, J.P.M., Harvey, N., Wolanski, E., Burnett, W.C., Perillo, G.M.E., Gornitz, V., Arthurton, C.R.K., Bokuniewicz, H., Campbell, J.W., Cooper, L., Dunton, K., Gao, S., Hesp, P.P., Saito, Y., Salisbury, J., Snoussi, M., Yim, W.W., 2005. Chapter 2 dynamics of the coastal zone. Coast. Change Anthropol. http://dx.doi.org/10.1007/3-540-27851-6.

Young, I.R., Babanin, A.V., Zieger, S., 2011. Global trends in wind speed and wave height. Science 332, 454–455. http://dx.doi.org/10.1126/science.1197219.